Biochimica et Biophysica Acta 1822 (2012) 970–979

Contents lists available at SciVerse ScienceDirect

Biochimica et Biophysica Acta

journal homepage: www.elsevier.com/locate/bbadis

Protein profiling reveals energy metabolism and cytoskeletal protein alterations in *LMNA* mutation carriers

Cinzia Magagnotti [a], Angela Bachi [a,b], Gianpaolo Zerbini [c], Elena Fattore [d], Isabella Fermo [e], Michela Riba [f], Stefano C. Previtali [g], Maurizio Ferrari [h,i,j], Annapaola Andolfo [a,*,1], Sara Benedetti [h,1]

[a] *ProMiFa, Protein Microsequencing Facility, Division of Cell Biology and Genetics, San Raffaele Scientific Institute, Milan, Italy*
[b] *Biological Mass Spectrometry Unit, Division of Cell Biology and Genetics, San Raffaele Scientific Institute, Milan, Italy*
[c] *Complications of Diabetes Unit, Division of Cardiovascular and Metabolic Sciences, San Raffaele Scientific Institute, Milan, Italy*
[d] *Department of Environmental Health Sciences, "Mario Negri" Institute for Pharmacological Research, Milan, Italy*
[e] *Division of Immunology, Transplantation and Infectious Diseases, San Raffaele Scientific Institute, Milan, Italy*
[f] *Neurogenomics Unit, Center for Translational Genomics and Bioinformatics, San Raffaele Scientific Institute, Milan, Italy*
[g] *Division of Neuroscience and Institute of Experimental Neurology (INSPE), San Raffaele Scientific Institute, Milan, Italy*
[h] *Laboratory of Molecular Biology, Diagnostica e Ricerca San Raffaele, San Raffaele Scientific Institute, Milan, Italy*
[i] *Vita-Salute San Raffaele University, Milan, Italy*
[j] *Genomic Unit for the Diagnosis of Human Pathologies, Center for Translational Genomics and Bioinformatics, San Raffaele Scientific Institute, Milan, Italy*

ARTICLE INFO

Article history:
Received 29 September 2011
Received in revised form 21 December 2011
Accepted 27 January 2012
Available online 3 February 2012

Keywords:
Laminopathies
Mass spectrometry
Muscular dystrophy
Proteomics
Skin fibroblasts

ABSTRACT

Nuclear envelope-related muscular dystrophies, in particular those referred to as laminopathies, are relatively novel and unclear diseases, also considering the increasing number of mutations identified so far in genes of the nuclear envelope. As regard *LMNA* gene, only tentative relations between phenotype, type and localization of the mutations have been established in striated muscle diseases, while laminopathies affecting adipose tissue, peripheral nerves or progerioid syndromes could be linked to specific genetic variants. This study describes the biochemical phenotype of neuromuscular laminopathies in samples derived from *LMNA* mutant patients. Since it has been reported that nuclear alterations, due to *LMNA* defects, are present also in fibroblasts from Emery–Dreifuss muscular dystrophy and familial partial lipodystrophy patients, we analyzed 2D-maps of skin fibroblasts of patients carrying 12 different *LMNA* mutations spread along the entire gene. To recognize distinctive proteins underlying affected biochemical pathways, we compared them with fibroblasts from healthy controls and, more importantly, fibroblasts from patients with non-lamin related neuromuscular disorders. We found less abundance of cytoskeletal/structural proteins, confirming a dominant role for Lamin A/C in structural support of nuclear architecture. Interestingly, we also established significant changes in the expression of proteins involved in cellular energy production and oxidative stress response. To our knowledge, this is the first report where proteomics was applied to characterize ex-vivo cells from *LMNA* patients, suggesting that this may represent a new approach to better understand the molecular mechanisms of these rare diseases and facilitate the development of novel therapeutic treatments.

1. Introduction

Alterations in the *LMNA* gene, encoding the nuclear envelope proteins Lamin A/C, lead to a heterogeneous spectrum of human diseases collectively denominated laminopathies, which can be classified into tissue-restricted or systemic disorders. The former includes Emery–Dreifuss and limb-girdle muscular dystrophies [1,2], Charcot–Marie–Tooth neuropathy [3], dilated cardiomyopathy and conduction system defects [4], and Dunningan-type familial partial lipodystrophy [5]. The second group comprises developmental abnormalities with or without premature aging (mandibuloacral dysplasia, Hutchinson–Gilford and atypical Werner progeria syndromes, restrictive dermopathy [6–8]). Although some genotype–phenotype correlation has been attempted [9], these disorders display a striking intra-familiar and inter-familiar clinical heterogeneity, which may be partly ascribable to different genetic backgrounds.

However, in spite of more than 400 *LMNA* mutations described to date, the understanding of pathogenetic mechanisms involved in the different clinical forms of laminopathies remains incomplete, especially for neuromuscular subtypes. Several hypotheses have been proposed so far, reflecting the variety of cellular functions involving Lamin A/C. Firstly, Lamin A/C as type V nuclear intermediate filament proteins, is involved in the structural support of nuclear architecture. *LMNA* mutations may therefore increase nuclear fragility, disrupting

* Corresponding author. Tel.: +39 02 26432714; fax: +39 02 26436585.
E-mail address: annapaola.andolfo@hsr.it (A. Andolfo).
[1] These authors equally contributed.

0925-4439/$ – see front matter © 2012 Elsevier B.V. All rights reserved.
doi:10.1016/j.bbadis.2012.01.014

the mechanical coupling between the cytoskeleton and the nucleus and consequently leading to a greater susceptibility to physical stress, especially in tissues exposed to mechanical strain such as skeletal and cardiac muscle [10,11]. Lamin A/C defects can also affect different nuclear functions such as DNA replication, RNA transcription and maturation [12] by interacting with chromatin and with several transcription factors [13]. In addition, Lamin A/C is also involved in a variety of signaling pathways affecting cell growth and differentiation, including MAPK, TGFβ, Notch, pRb and MyoD [14–17]. It has been recently suggested that muscle atrophy may also depend on defects in the neuromuscular junction secondary to synaptic nuclei mispositioning [18]. Finally, it is now believed that *LMNA* mutations primarily affect not only myofibers but also the efficiency of satellite cells in muscle repair and regeneration [19].

Many studies have demonstrated that Lamin A/C defects induce changes in nuclear morphology in a subset of cells, like misshapen nuclei, nuclear pores clustering, mislocalization of associated proteins and aberrant intranuclear lamin foci [20]. However, the relevance of these abnormalities and their possible pathogenetic mechanism is still unclear, since no obvious links have been established with the heterogeneous clinical phenotypes.

Proteomic studies have been increasingly used to obtain a comprehensive and unbiased characterization of human disorders because of their capability to detect both qualitative and quantitative gene expression differences [21]. This kind of approach gives the opportunity to explore the entire proteome, revealing alterations in unexpected signaling pathways. For example, a recent proteomic profiling of heart in a mouse model of Duchenne muscular dystrophy identified 29 differentially expressed proteins mainly involved in energy metabolism and contractile machinery, previously not correlated to the disease [22].

Our approach aimed at describing the biochemical phenotype of neuromuscular laminopathies, in order to improve our knowledge on the molecular pathways involved in Lamin A/C diseases. Skin fibroblasts from *LMNA* mutation carriers with personal or family history of skeletal or cardiac muscle disorder were subjected to proteomic analysis to identify differentially expressed proteins compared to controls. Gene Ontology and Principal Component Analysis (PCA) with Western Blot (WB) validation suggested that *LMNA* defects affect primarily the expression of proteins involved in cytoskeleton organization, energy metabolism and oxidative stress response, even when compared to other neuromuscular diseases. To our knowledge, this is the first study where a combination of proteomics procedures was applied to characterize *LMNA* patient samples.

2. Materials and methods

2.1. Materials

Trypsin-EDTA, minimum Eagle's medium and fetal calf serum were purchased from Gibco, Invitrogen (Carlsbad, CA, USA). Dimethyl sulfoxide, PBS, bovine serum albumin (BSA), urea, thiourea, protease inhibitors, trizma base, glycine, CHAPS, 1,4-dithioerythritol (DTE), iodoacetamide, alpha-cyano-4-hydroxycinnamic acid, mouse monoclonal Alpha-Tubulin (used at 1:1000 v/v dilution) and Actin antibody (used at 1:5000 v/v dilution) were from SIGMA Chemical Company (St. Louis, MO, USA). Phosphatase inhibitors were from CalBiochem (San Diego, CA, USA). Zwittergent, Destreak, IPG buffer, Immobiline dry strips pH 3-10NL 13 cm, mineral oil, Hybond-ECL nitrocellulose membrane, ECL detection kit and appropriate HRP-conjugated secondary antibodies were from GE Healthcare (Uppsala, Sweden). Acrylamide 30% solution and Colloidal Brilliant Blue Coomassie were from BioRad Laboratories (Hercules, CA, USA). Trypsin sequencing grade was from Roche Diagnostics (Mannheim, Germany). Goat polyclonal Lamin A/C (N-18) antibody (used at 1:1000 v/v dilution) was from Santa Cruz Biotechnology (Santa Cruz, CA, USA). Rabbit polyclonal Alpha B Crystallin antibody (used at 1:200 v/v dilution) was from Covance (Princeton, NJ, USA). Goat polyclonal Triosephosphate Isomerase antibody (used at 1:5000 v/v dilution) was from Abcam Ltd. (Cambridge, UK).

2.2. Methods

2.2.1. Clinical evaluation

Ethics approval for this study was obtained by the San Raffaele Institute Ethics Committee (protocol LMNA-02). The investigation conformed with the principles outlined in the Declaration of Helsinki. Patients underwent complete neurological and cardiological examination. Neurological assessment included evaluation of muscle weakness, presence of contractures, functional disability, progression of disease, electromyography and determination of serum creatine kinase levels. Cardiological assessment included 12-leads electrocardiogram, echocardiogram, 24 hour-Holter monitoring, heart magnetic resonance imaging with injection of paramagnetic contrast medium and, in the absence of serious neurological impairment, ergometric test.

2.2.2. Genetic analysis

Written informed consent was obtained before genetic analysis. Genomic DNA extraction, PCR amplification, denaturing high pressure liquid chromatography and direct sequencing of *LMNA* gene were performed as previously described [23]. Primer sequences and reaction conditions are available upon request. *LMNA* reference sequences were NCBI NG_008692.1 for genomic DNA, NCBI NM_170707 for lamin A cDNA and NCBI NM_005572 for lamin C cDNA. Nucleotides were numbered starting from ATG.

2.2.3. Skin biopsies and fibroblast culture

A skin specimen of approximately 2 mm^3 was taken by excision under local anesthesia from an avascular area of the anterior aspect of forearm of 30 patients and 3 healthy controls. Fibroblasts were split with trypsin-EDTA 0.25% and progressively expanded in 60 mm culture dishes in minimum Eagle's medium (MEM) supplemented with 10% fetal calf serum. At the fourth passage in culture, $2–3*10^6$ fibroblasts were harvested, resuspended in MEM supplemented with 30% fetal calf serum and 5% dimethyl sulfoxide (freezing medium) and frozen in liquid nitrogen in several aliquots for future experiments. Skin fibroblasts, expanded in 7 passages up to $10*10^6$, were detached with trypsin-EDTA 0.25%, washed twice with ice-cold PBS and divided in two aliquots and stored at −80 °C until analysis.

2.2.4. Proteomic analysis

2.2.4.1. Cell lysis. Skin fibroblast samples were lysed for 40 min on mixing wheel at 4 °C in 400 μl of lysis buffer (5 M urea, 2 M thiourea, 2% CHAPS w/v, 2% Zwittergent v/v, protease and phosphatase inhibitors). The lysates were centrifuged at 14,000 rpm for 15 min at 15 °C and stored at −80 °C. The recovered supernatant was analyzed to determine total protein concentration using BioRad protein assay and BSA as standard.

2.2.4.2. Two-dimensional gel electrophoresis. For 2D electrophoresis, 300 μg total proteins were loaded on each gel and each sample was run in triplicates. Prior to the first dimension of isoelectric focusing, each sample was added of Destreak (final concentration: 100 mM) and IPG buffer (final concentration: 0.5%) and then run at 100,000 V h on 13 cm strips, with a non linear gradient pH 3–10. The second dimension was SDS–PAGE 10%, stained with Colloidal Brilliant Blue Coomassie, upon reduction with DTE and alkylation with iodoacetamide of the strips. We intentionally used CBB as protein stain, because it is very cheap, really reproducible and it is

characterized by a greater linear dynamic range compared to Silver staining [24].

2.2.4.3. Gel image analysis. Gel images were acquired by ProXPRESS 2D Proteomic Imaging System and quantitative comparisons of spot intensities were carried out using Progenesis SameSpots (Nonlinear Dynamics, Newcastle upon Tyne, UK). Background subtraction and spot intensity normalization were automatically performed by Progenesis SameSpots. Relative spot intensity values were calculated on a logarithmic scale and converted to relative fold-difference levels. Statistical analysis was also automatically performed by Progenesis SameSpots on intensity values of protein spots from three separate gels for each sample. Differential spots, characterized by a fold-change ≥ 1.5 and p-value < 0.05, were identified by in-gel digestion followed by MALDI-TOF or nLC-ESI mass spectrometry analysis.

2.2.4.4. In-gel digestion and mass spectrometry analysis. The spots of interest were manually excised from the gels, destained, sequentially reduced and alkylated, and digested overnight with sequencing-grade modified trypsin, as previously described [25]. Aliquots of the sample containing tryptic peptides were directly analyzed by MALDI-TOF/MS for peptide mass fingerprinting (PMF) analysis [26]. Peptide mass lists, obtained after deisotoping, were submitted to UniProtKB 2010_11 (12898884 sequences; 4176319342 residues) using the MASCOT peptide mass fingerprint program (version 2.2.07, Matrix Science, UK). The main search parameters were: taxonomy: *Homo sapiens*; one missed cleavage allowed; carbamidomethylation of cysteine as fixed modification; oxidation of methionine as variable modification; mass tolerance of 50 ppm. Alternatively, tryptic peptides were analyzed by nLC-ESI-MS/MS as already reported [27], generating amino acid sequence information too for protein identification. All MS/MS samples were analyzed using MASCOT engine to search the UniProtKB 2010_11 (12898884 sequences; 4176319342 residues). We used a peptide mass tolerance of 200 ppm and 0.3 Da for precursor and fragment ions, respectively. Searches were performed with trypsin specificity, alkylation of cysteine by carbamidomethylation as fixed modification, and oxidation of methionine as variable modification.

2.2.4.5. Western blot analysis. 40 μg total cellular proteins were separated on SDS-10% polyacrylamide gel. Resolved proteins were electrotransferred onto Hybond-ECL nitrocellulose membrane with an ECL Semidry Blotter TE 77 PWR apparatus (GE Healthcare) for 1 h at 0.8 mA/cm^2 in transfer buffer (25 mM trizma base, 40 mM glycine, 20% methanol, 0.05% SDS). Membranes were probed for Lamin A/C, Triosephosphate isomerase, Alpha B Crystallin, Actin and Alpha-Tubulin. Detection was by enhanced chemiluminescence (ECL) reaction (ECL detection kit, GE Healthcare) and proteins were visualized on autoradiography films (Hyperfilm ECL, GE Healthcare). Densitometry values were determined using ImageJ 1.45e software.

2.2.5. Bioinformatic analysis

2.2.5.1. Heatmap building. The heatmap was generated by Stanford software Heatmap builder version 1.0 freely available to the academic community (http://ashleylab.stanford.edu/tools_scripts.html). Heatmap is presented as row normalized (maximum and minimum values are calculated for each spot) ink-blot [28].

2.2.5.2. BiNGO (Biological Networks Gene Ontology). The proteins identified in this study were analyzed according to the three organizing principles of Gene Ontology (GO: http://www.geneontology.org: BP: Biological Process, MF: Molecular Function, CC: Cellular Component), using the bioinformatic tool BiNGO v. 2.44, as a plug-in of Cytoscape v. 2.8 [29]. BiNGO is an open-source Java tool to determine which GO terms are significantly over-represented in a test set of proteins. We used gene ontology.obo v.1.2 as reference set, GOSlim generic as ontology file, a p-value threshold of 0.05 and *Homo sapiens* taxonomy. Hypergeometric test with Benjamini and Hochberg correction for FDR was applied. Indeed, we could determine not only the frequency of each category for ours and reference set but also the ratio of these two values, thus obtaining an indication of over-represented GO categories in our proteins. Moreover, as regard the MF ontology, BiNGO permitted us to build a graph where over-represented children categories are reported as nodes. The area of each node is proportional to the number of proteins in the test set annotated to the corresponding GO category. Color code of the nodes indicates the statistical significance.

2.2.5.3. Principal Component Analysis. Data were analyzed using Principal Component Analysis (PCA), a multivariate projection method designated to extract and highlight the systematic variation into a multivariate data matrix. The method allows to investigate the original data using a smallest number of variables (the principal components), while preserving the greatest possible amount of information [30]. As a consequence, data can be represented in a bi- tri-dimensional plot which makes easy to visualize similarities, clusters or trend in the original data.

The data matrix was constituted from N rows (19 biological samples, including 18 *LMNA* mutation carriers versus all the neuromuscular disease controls collapsed in one) and K columns (73 spots). Before the analysis, since the large difference in the variables' numerical range, data were scaled to unit variance and mean-centered; in addition some variables, which were markedly skewed, were log transformed. The analysis was carried out using Simca-P 8.0 (Umetrics AB, Umeå, Sweden) software.

3. Results

3.1. Patient clinical and genetic characterization

Our cohort included 18 *LMNA* mutation carriers (Table 1). Thirteen of these were initially referred to our center for neurological disease, including limb-girdle (LGMD-1B) or Emery–Dreifuss (EDMD) muscular dystrophies and peripheral neuropathy, while five asymptomatic *LMNA* mutation carriers were identified during family studies.

LMNA mutations comprised seven missense substitutions, one frameshift and one in-frame deletion and one splice donor site alteration. In addition, two silent substitutions not leading to amino acid change were included. Their presence in the normal population was excluded by analysis of 180 healthy chromosomes. Variants were scattered along the entire Lamin A/C protein, including head, coiled coil, Ig fold and tail domains (Table 1).

Careful cardiological evaluation revealed in many cases a concomitant cardiac phenotype, characterized by dilated cardiomyopathy (DCM), ventricular and supraventricular arrhythmias and conduction defects.

To investigate pathways involved in the pathogenesis of Lamin A/C-related neuromuscular disorders, we undertook a pilot protein profiling study. Control groups included 12 patients affected by myopathy or muscular dystrophy not related to *LMNA* mutations (neuromuscular disease controls) and 3 unaffected subjects (healthy controls).

Among neuromuscular disease controls, one was affected by Becker muscular dystrophy, three by limb-girdle muscular dystrophy, one Bethlem and one desmin myopathy, two distal myopathies, three metabolic myopathies and one peripheral neuropathy.

3.2. Protein profiling of human skin fibroblasts from LMNA patients versus healthy controls

In order to identify differentially expressed proteins in *LMNA* mutation carriers ($N = 18$) versus healthy subjects ($N = 3$), skin biopsies were performed and fibroblasts were isolated as described in the Methods section. Fibroblast lysates were separated using 2D

Table 1
Clinical and genetic characterization of *LMNA* mutation carriers. Year of birth for each patient is reported. *LMNA* mutations at DNA and protein level are described. Both neurological and cardiac phenotypes are depicted.

Patient #	Year of birth	*LMNA mutation (DNA)*	*LMNA mutation (protein)*	Domain	Neurological phenotype	Cardiac phenotype
L-206	1979	c.31delC	p.R11AfsX83	Head	LGMD, TC	VEB, SVEB
L-1224	1951	c.99G>C	p.E33D	Head	LGMD, TC	DCM, AF
L-218	1988	c.99G>C	p.E33D	Head	Asymptomatic	Asymptomatic
L-214	1982	c.99G>C	p.E33D	Head	Asymptomatic	INITIAL ARVD
L-216	1951	c.194A>G	p.E65G	Coil 1A	LGMD, TC	AVB, AF
L-227	1979	c.194A>G	p.E65G	Coil 1A	LGMD, TC	INITIAL ARVD
L-232	1960	c.471G>A	p.T157T	Coil 1B	LGMD, TC	?
L-234	1959	c.565C>T	p.R189W	Coil 1B	LGMD, PN	DCM
L-222	1977	c.1039G>A	p.E347K	Coil 2B	Asymptomatic	INITIAL ARVD
L-235	1955	c.1380+1G>A	Splicing alteration	Ig fold	LGMD, TC	DCM
L-219	1975	c.1357C>T	p.R453W	Ig fold	LGMD, TC	AF
L-204	1961	c.1368_70delCAA	p.N456del	Ig fold	LGMD, TC	DCM, AF
L-203	1989	c.1368_70delCAA	p.N456del	Ig fold	EDMD	Asymptomatic
L-208	1955	c.T1535>C	p.L512P	Ig fold	LGMD, TC	AVB, NSVT
L-230	1984	c.T1535>C	p.L512P	Ig fold	Asymptomatic	Asymptomatic
L-190	1983	c.1683G>C	p.L561L	Tail	PLD, PN	?
L-237	1949	c.1711C>T	p.R571C	Tail	Asymptomatic	INITIAL ARVD
L-236	1989	c.1711C>T	p.R571C	Tail	EDMD, PN	Asymptomatic

Legend: AF atrial fibrillation; ARVD arrhythmogenic right ventricular dysplasia; AVB atrio-ventricular block; DCM dilated cardiomyopathy; EDMD Emery–Dreifuss muscular dystrophy; LGMD limb-girdle muscular dystrophy; NSVT nonsustained ventricular tachycardia; PLD partial lipodystrophy; PN peripheral neuropathy; SVEB supraventricular ectopic beats; TC tendon contractures; VEB ventricular ectopic beats.

electrophoresis. Representative 2D gels of healthy skin fibroblasts (panel a) and *LMNA* patient fibroblasts (panel b) are reported in Fig. 1. Each sample was run in triplicate in order to obtain a statistically significant image analysis of the spot intensities. We were able to retrieve a total of 539 spots (data not shown) and we decided to define as differentially displayed spots those with a fold-change threshold ≥ 1.5 and a p-value < 0.05. In order to be sure that we were looking at relevant proteins, we focused our attention on proteins whose expression resulted to be concordantly changed in at least two patients. This criterion permitted us to reduce the number of differential spots up to 66, which were digested and analyzed by mass spectrometry. Protein identities, pI, MW, sequence coverage, number of matched peptides/measured peptides or fragmented peptides and Mascot scores are reported in Additional file A.

Forty-eight unique proteins were grouped according to Gene Ontology (GO) terminology, using the bioinformatic tool BiNGO. A graphical description of the over-represented GO terms in our test set of proteins is given in Additional file B (p-value < 0.05). In the graph, protein categories are displayed according to their decreasing statistical significance. We found an enrichment of altered proteins involved in metabolic processes, including carbohydrate metabolic process and generation of precursor metabolites and energy (Additional file B, panel a). The same graph illustrates an over-representation of structural/cytoskeletal proteins. Indeed, when deeply analyzing the molecular function ontology, we established protein binding category as predominantly represented. Proteins assigned to this category were involved in cytoskeletal protein binding and, more specifically, in actin binding (Additional file B, panel b). This finding was not surprising, considering that we were looking for proteins altered in cells derived from patients affected by neuromuscular diseases; however, we could not conclude whether the observed effects on protein expression were specifically related to *LMNA* defects or were a general consequence of neuromuscular disease.

3.3. Protein profiling of human skin fibroblasts from LMNA mutation carriers versus neuromuscular disease controls

In order to understand whether our list of differentially expressed proteins represented a specific effect of *LMNA* mutations or a general phenotype of neuromuscular diseases, we subsequently compared protein profiles of skin fibroblasts from *LMNA* patients to those ones derived from other myopathies as controls. Representative 2D gels of neuromuscular disease control fibroblasts (panel a) and *LMNA* patient fibroblasts (panel b) are reported in the Additional file C. Fig. 2 shows the heatmap in which the fold-changes (≥ 1.5 and p-value < 0.05) for each spot and in each patient are reported. The identity of proteins, as revealed by mass spectrometry analyses, is also listed (MS details are given in the Additional file D). Using the same criteria reported above, we identified 47 unique proteins out of 73 analyzed spots. As reported in Fig. 3, BiNGO analysis was very similar to that obtained from the comparison of patients with healthy controls (see Additional file B). Again, we could observe that the most affected proteins were cytoskeletal/structural proteins and enzymes related to carbohydrate metabolism. This data could suggest that the altered protein expression was not a general consequence of the presence of neuromuscular diseases, rather a specific effect of *LMNA* defects. Moreover, a remarkable enrichment was observed for the oxidative stress response activity (Fig. 3, panel a: ratio = 17.61). This data was further evident in the children graph (Fig. 3, panel b), where oxidoreductase activity was significantly over-represented, according to the color code for nodes.

3.4. Clustering of LMNA patients according to their protein profile

As reported in Table 1, our *LMNA* patients are characterized by different point mutations manifesting in a quite heterogeneous scenario of clinical phenotypes. Nevertheless, we found that the same proteins were differentially expressed in some patients. In order to define which proteins, if any, could discriminate/cluster our patients, we ran PCA on the data matrix containing the normalized spot volume, as measured by SameSpots software, for the differentially expressed proteins in each *LMNA* patient versus neuromuscular disease controls. Results of the PCA (Fig. 4) showed that the first and second components respectively explained 24% and 17% of the variability of the original data set, which was a quite good result for such complex biological samples. The score plot (Fig. 4, panel a) revealed a gathering of some patients, for example: L-208 and L-206 (group 1); L-232, L-230, and L-227 (group 2); and L-236, L-190, L-234, L-219 and L-235 (group 3). However, the control sample, which was composed by all the neuromuscular disease controls, was scattered in the central part of the graph close to other samples bearing *LMNA* mutations (from now on, named scattered patients).

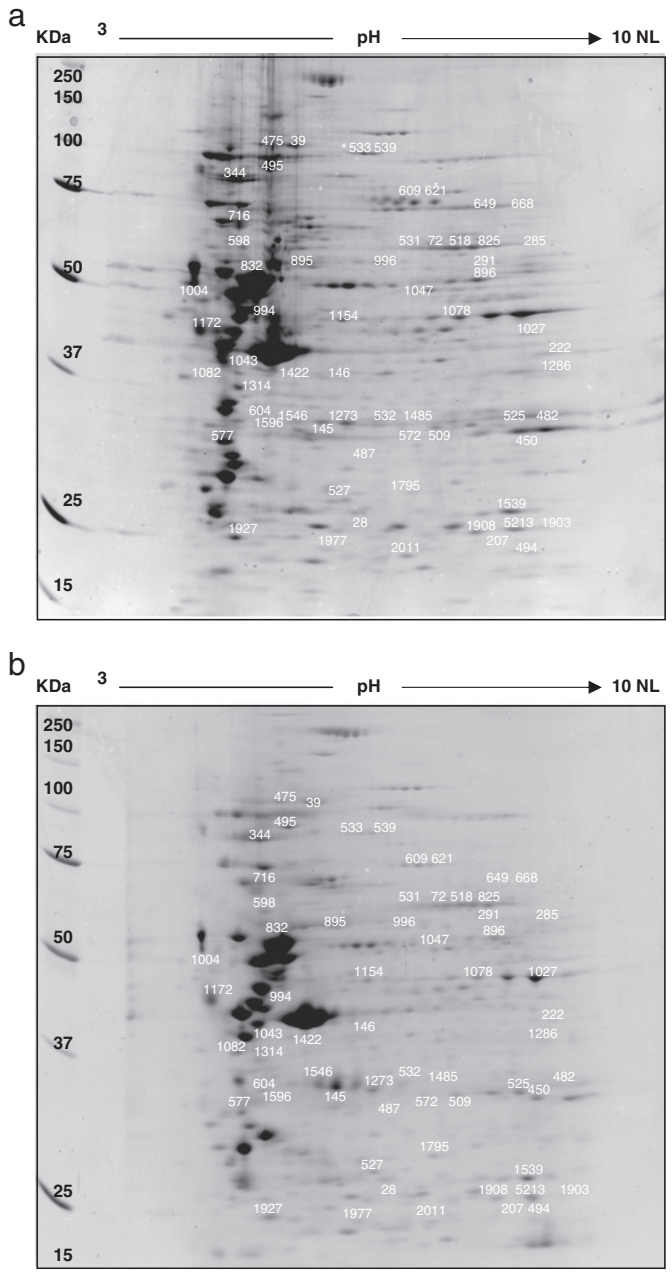

Fig. 1. Representative 2D gels of human skin fibroblast lysate. 300 μg total proteins were loaded on 10% SDS–PAGE. The gels were stained with Colloidal Brilliant Blue Coomassie. MW and pH range are indicated. Differentially displayed spots in *LMNA* mutation carriers (panel b) versus healthy donors (panel a) are marked by numbers, as reported in the Additional file A.

Proteins determining the clustering of the samples in Fig. 4 (loading plot, panel b), include: Lamin A/C (spots: 518, 649, 667), cytoskeletal/structural proteins (Caldesmon, spots: 433, 434, 609, 611, 621; Alpha-Actinin 1, spot: 474; PDZ and LIM domain 1, spot: 525; Septin 11, spot: 1078; Alpha B Crystallin, spot: 2051) and proteins involved in metabolic processes (Phosphoglycerate kinase 1, spot: 1286; Triosephosphate Isomerase, spot: 5213) (see Additional file D).

Due to the heterogeneity of *LMNA* mutation carriers (both at level of mutation localization and clinical phenotype) and to the small number of examined patients (however, we are analyzing a rare disease), no clear gathering of patients was expected. Actually, we also tried to use other variables to cluster our patients, but neither clinical phenotype, nor disease onset nor point mutation localization in recognized lamin domains gave rise to any reliable patient stratification (data not shown). Therefore, our finding is indicating that, apart the above mentioned limits of this study, the protein profiling of ex-vivo cells is a promising way to try to stratify patients.

3.5. Validation by semi-quantitative WB analysis

In order to uncover fine differences among the groups, which resulted from the PCA analysis, we further investigated three different proteins by WB in a semi-quantitative way: Lamin A/C, Triosephosphate Isomerase and Alpha B Crystallin. These proteins, not only were the most relevant for patients' clustering (Fig. 4), but were also representative of the most altered protein categories as revealed by BiNGO results.

Skin fibroblast lysates from two random patients in each group and three random neuromuscular disease controls were analyzed in triplicates by WB; protein content was normalized to Alpha-Tubulin signal. Fig. 5 refers to a representative WB for the investigated proteins and to the graphical box-plot representation of the densitometric analyses. Protein fold-changes, as obtained by comparing each group to neuromuscular disease controls, are reported. Overall, WB analysis not only permitted us to validate our results, but also to highlight statistically significant differences among the recognized groups, suggesting that not a single protein but, most likely, a panel of proteins might better cluster our patients. In details, for Lamin A/C we found a p-value <0.05 in all pairwise comparison between groups, except for Group 1 versus Group 3. As regard Triosephosphate Isomerase, only the scattered patient group resulted to be statistically different from the others; finally, Alpha B Crystallin was significantly reduced in all the groups except for Group 3 (Fig. 5, panels a, c and d, respectively).

It is noteworthy that Actin, initially used to normalize the amount of protein loaded in the WB, was unexpectedly found to be not equally abundant in our samples: indeed, it was significantly decreased in group 2 and scattered patients (Fig. 5, panel b). Even if unpredicted on the basis of Progenesis SameSpots analysis, this result confirms our findings on the changes induced on cytoskeletal proteins. The discrepancy between Progenesis SameSpots and WB analyses can be explained considering the major sensitivity of the WB that uses a specific antibody directed against Actin.

4. Discussion

This work shows for the first time the use of a proteomics approach to describe proteome-wide changes in *LMNA* mutation carrier samples. So far, different cell culture models [31–33] or mouse models [34] have been created to better understand the pathogenesis of laminopathies, but here we present the first proteomics data on patients. Findings of our study suggest that different pathways concur to determine Lamin A/C neuromuscular diseases.

12 different *LMNA* mutations were included, scattered along the entire protein sequence (Table 1) and thus not focusing on a particular molecular defect that could justify the disease. This cohort presented a heterogeneous scenario of clinical phenotypes from LGMD-1B to EDMD muscular dystrophy, to dilated cardiomyopathy. Within our cohort of patients, as also reported in literature [35], we observed that the same *LMNA* mutation can cause diverse clinical phenotypes (i.e. L-203 and L-204, Table 1), even including asymptomatic subjects (i.e. L-218 and L-230, Table 1). Therefore, our hypothesis was that not only lamin mutation but also other factors/proteins can explain the disparate disease manifestations, which are not restricted to one tissue/organ. Indeed, while not being the primary affected tissue, it has been reported that nuclear alterations due to *LMNA* mutations are also present in fibroblasts from Emery–Dreifuss muscular dystrophy and familial partial lipodystrophy patients [36]. In addition, mouse embryonic fibroblasts lacking Lamin A/C, display a "fragile" nucleus [37] and anomalies affecting cytoskeletal organization [38] and, as also very recently shown, cytoskeleton-based cell functions [39]. All together, these previous studies and the easier availability

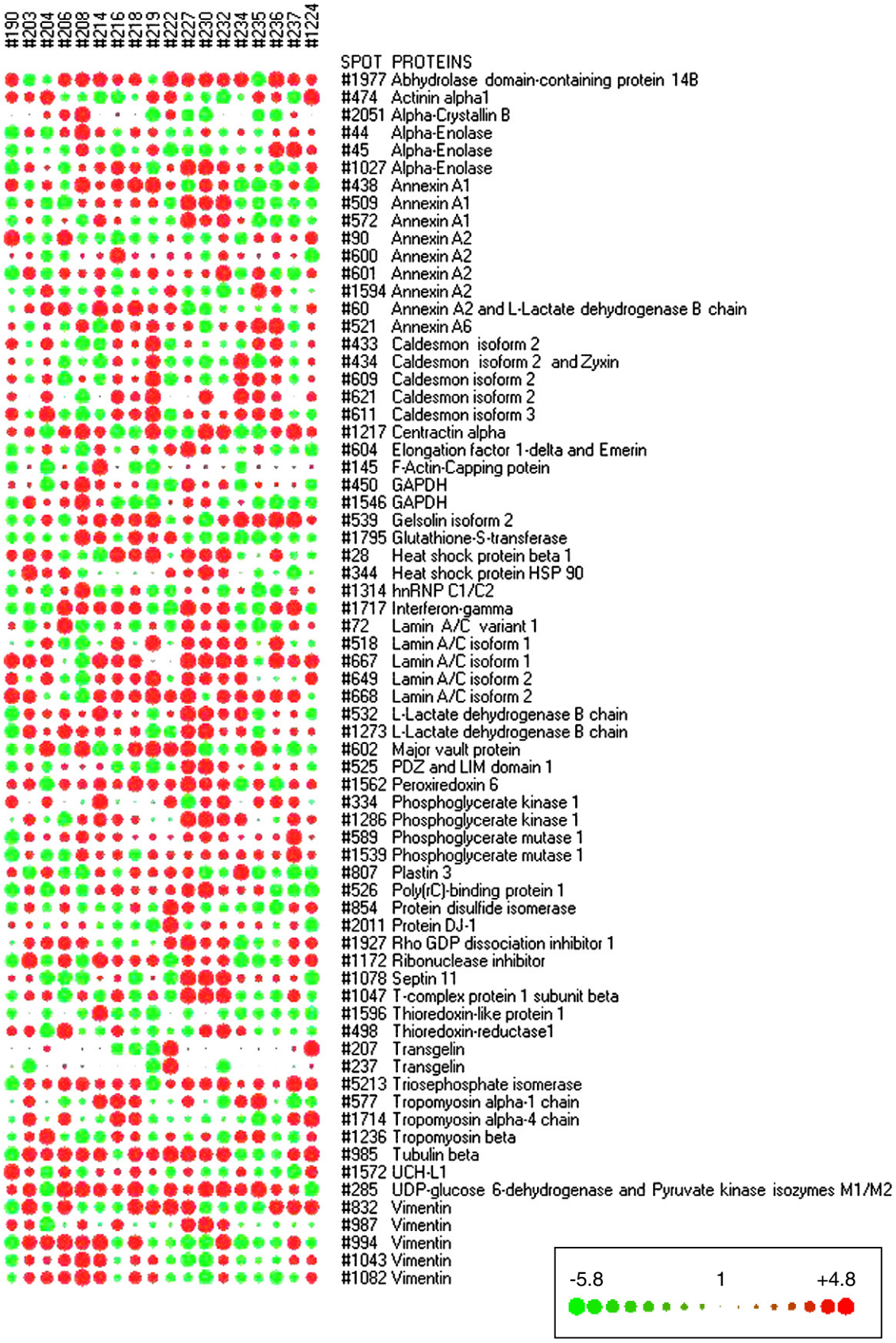

Fig. 2. Heatmap of spots differentially displayed in human skin fibroblasts from *LMNA* mutation carriers versus neuromuscular disease controls. The reported spots showed a fold-change ≥ 1.5 and a p-value <0.05. The color and size of dot indicates the different extent of more and less abundance. The larger size of the dot signifies the greater discrepancy in expression level between *LMNA* patients and neuromuscular disease controls. Identities of proteins are reported according to the mass spectrometry results (see Additional file D).

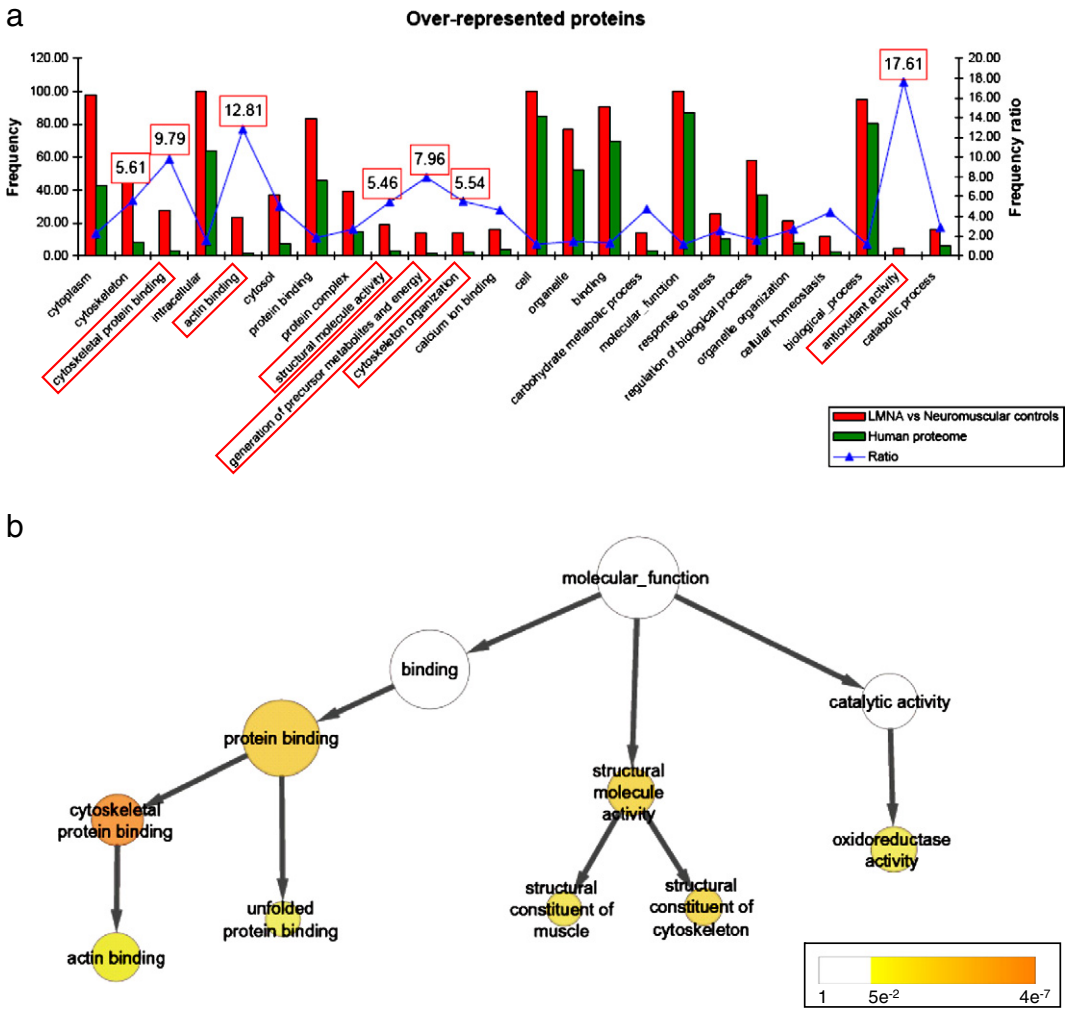

Fig. 3. BiNGO analysis of human skin fibroblasts from *LMNA* mutation carriers versus neuromuscular disease controls. Diagram refers to over-represented GO categories (as listed in GOSlim generic) in our set of proteins, as compared to *Homo sapiens* proteome, using ontology.obo v.1.2 as reference set. The principal Y-axis refers to the frequency of each GO term (x/X for our set or n/N for the reference set), while the secondary Y-axis refers to the ratio x/X/n/N (panel a). The graph reports the over-represented GO categories, which are children of molecular function term (panel b). The color code for statistical significance is indicated.

of skin fibroblasts compared to muscular biopsy, supported our hypothesis that fibroblasts may constitute a good candidate to evaluate the effects of Lamin A/C mutations. We thus analyzed protein profiles of skin fibroblasts derived from patients and controls, to determine specific alterations that could distinguish *LMNA* diseases from other neuromuscular disorders. In the future, the extension of results obtained from fibroblasts to muscular samples should permit to validate our results.

Firstly, we identified a subset of differentially expressed proteins in *LMNA* mutation carriers versus healthy controls (Additional file A). However, since some proteins may be non-specifically linked to disease progression, we subsequently compared protein profiles of Lamin A/C patients with those of patients with other neuromuscular disorders and no alteration in the *LMNA* gene (Additional file D). We singled out commonly altered proteins, which could suggest the affected biochemical pathways, even in distinct lamin mutation carriers. The list of identified proteins derived from the selection of statistically significant changes (fold-change ≥ 1.5 and p-value<0.05) observed in at least two patients (Additional files A and D). We adopted the criterion of two patients because, on one hand, we wanted to balance the inter-individual variability, but on the other, we knew that the mutations are distinct and rare, so that we could not be too restrictive. Moreover, as discussed above, since the same mutation can give rise to different clinical phenotypes, we could not expect to find so many common changes induced by different *LMNA* mutations.

Upon comparison between *LMNA* patients and neuromuscular disease controls, we obtained 73 differentially displayed spots, corresponding to 47 unique proteins. It has to be highlighted that the number of spots is different from the number of the identified unique proteins, as several spots are generated by the same protein likely carrying different post-translational modifications, which can explain the heterogeneity for each protein.

Among the others, we found that several spots related to Lamins A and C were differentially expressed in our patients. These findings can be ascribed to the effect of point mutations on the numerous post-translational modifications, known to be present on lamins [40]. These results were also confirmed when we compared the Lamin A/C level in patients' groups by WB analysis (Fig. 5, panel a).

The unique proteins were deeply studied according to their GO annotations, in order to delineate the altered pathways in our patients. BiNGO enrichment analysis (Fig. 3, panel a) suggested that *LMNA* defects affect specifically the expression of proteins involved in cytoskeleton organization, glucose metabolism and response to oxidative stress. Defects in structural support of nuclear architecture caused by *LMNA* mutations had been previously suggested [10,11,41]. According to this hypothesis, Lamin A/C defects may increase nuclear fragility and reduce cytoplasmic elasticity, disrupting

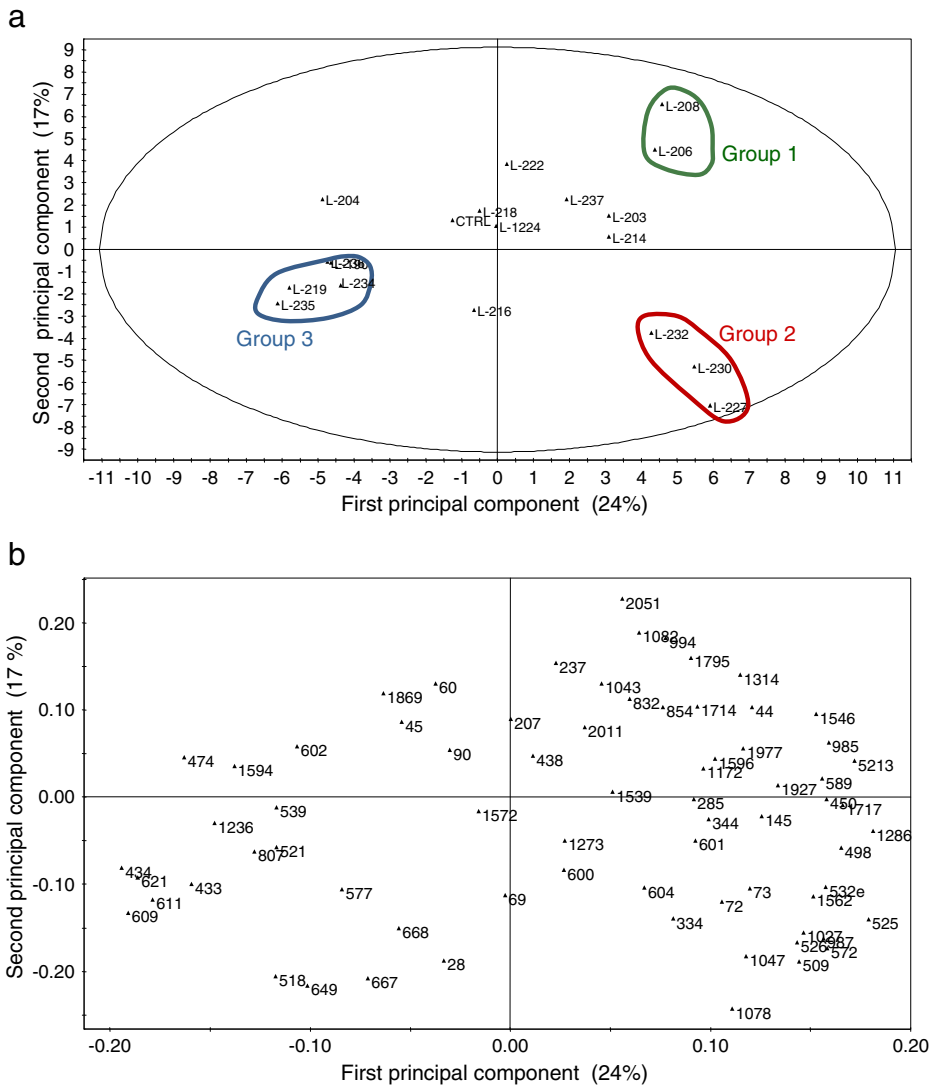

Fig. 4. Principal component analysis (PCA) of human skin fibroblasts from *LMNA* mutation carriers versus neuromuscular disease controls. The score plot (panel a) shows the biological samples into the space of the first and second principal components, which account, respectively, for 24 and 17% of variability of the original data set. The loading plot (panel b) indicates the spots distribution which determines the gathering of *LMNA* patients.

the mechanical coupling between the cytoskeleton and the nucleus provided by the LINC complex (LInker of Nucleoskeleton and Cytoskeleton) interacting with cytoskeletal networks. This may consequently lead to a greater susceptibility to physical stress, especially in tissues exposed to mechanical strain such as skeletal and cardiac muscle. In addition, it has been recently proposed that Lamin A/C mutations affect nuclear movement and positioning by impairing the anchorage of transmembrane actin-associated nuclear (TAN) lines attaching the nucleus to actin cables [39]. In this study, we detected differential expression of proteins involved in distinct cytoskeletal networks: actin microfilaments (Caldesmon, F-actin-capping protein, Gelsolin, Plastin 3, Tropomyosins, Zyxin); intermediate filaments (Vimentin) and microtubules (Tubulin beta) (Additional file D). We indeed observed a clear reduced expression of some cytoskeletal/structural proteins (Actinin alpha 1, Caldesmon, Plastin 3, Tropomyosins, and Vimentin), thus confirming the importance of cytoskeletal modifications in Lamin A/C related neuromuscular disorders (Fig. 2).

Our cohort of patients also revealed significant changes in the expression of proteins involved in cellular energy production. In many patients, we found less abundant glycolytic enzymes (Phosphoglycerate kinase 1, Triosephosphate Isomerase, Pyruvate kinase, Phosphoglycerate mutase 1, L-lactate dehydrogenase B chain), consistent with a previous report on HeLa cells with depleted expression of Lamin A/C [42]. In that study, the reduced (residual 9%) expression of lamins induced a decrease of metabolic enzymes (specifically, Triosephosphate Isomerase). A recent work demonstrated alterations of glycolysis in a limb-girdle muscular dystrophy patient showing down-regulation of glycolysis genes, thus suggesting an intrinsic defect in skeletal muscle metabolism due to Lamin A/C dysfunction [43].

Muscle oxidative stress has been proposed as a pathogenetic mechanism for Duchenne muscular dystrophy, with dystrophin-deficient muscle cells clearly more susceptible to oxidative stress in vitro [44]. In addition, recent findings show that free radicals play an important role in cardiomyopathy in *mdx* mice. Fibrosis is a consequence of oxidative stress in multiple tissues, including the heart [44]. Pathological modifications in free radical production in dystrophic muscle could yield defects in regulatory systems that may underlie some of the complex pathology of muscular dystrophy. Nevertheless, it is still controversial whether oxidative damage is a significant pathogenic event in muscular dystrophies, or it is a consequence. Our data suggested an involvement of oxidative stress in the pathogenesis of Lamin A/C related muscular dystrophy and cardiomyopathy. In fact we found an altered expression of Thioredoxin like protein 1, Thioredoxin reductase 1 and Peroxiredoxin 6, which are all proteins implicated in protection against oxidative stress. Actually, an increased sensitivity to oxidative stress in *LMNA* patients had been previously suggested [45,46].

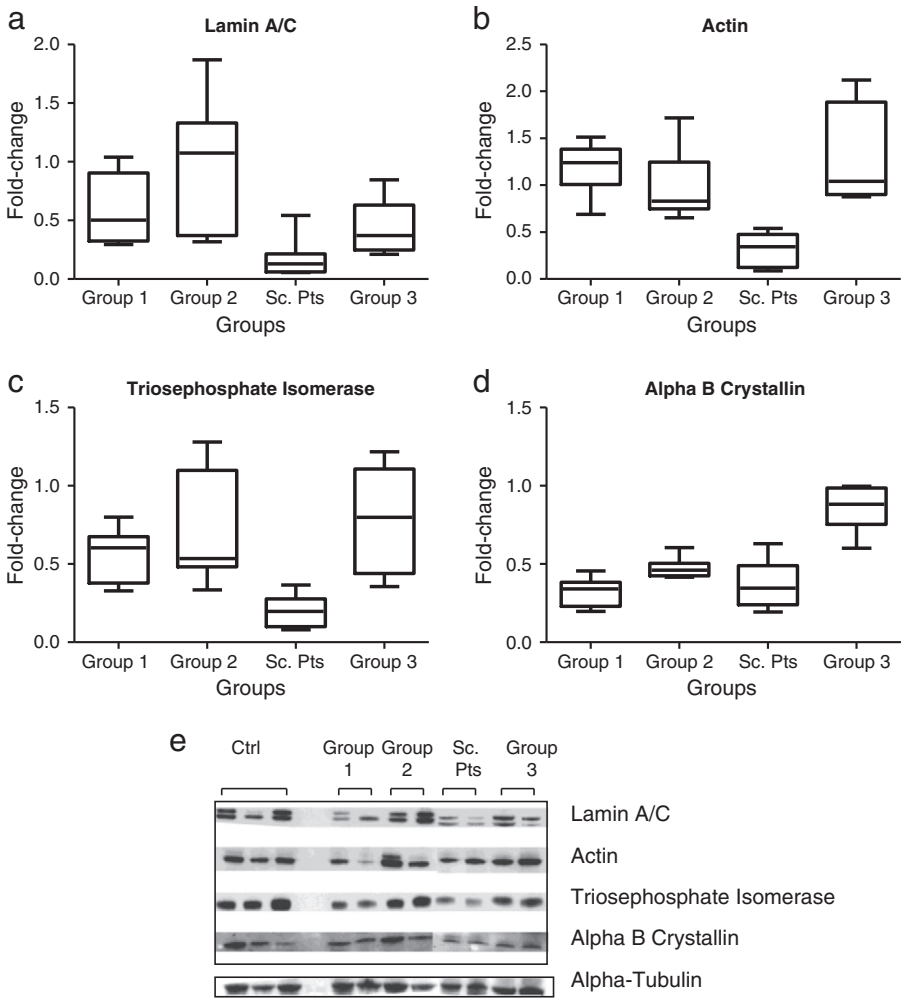

Fig. 5. Graphical box-plot representation of the densitometric WB analyses. Box plot of the fold-changes of Lamin A/C (panel a), Actin (panel b), Triosephosphate Isomerase (panel c) and Alpha B Crystallin (panel d) in human skin fibroblasts from *LMNA* mutation carriers versus neuromuscular disease controls. Boxes encompass the 25th and 75th percentiles; the horizontal line inside the box indicates the median. Whiskers extend to the 90th and 10th percentile. Representative WB for the investigated proteins are shown in panel e.

From our data, we can conclude that probably no single hypothesis can explain the variability of phenotypes associated with Lamin A/C defects and several molecular pathways likely concur to determine the pathological phenotypes. From the PCA (Fig. 4), our patients resulted to be divided into three major groups, considering both structural and carbohydrate metabolic enzymes as the most relevant proteins. This was evident in the loading plot (Fig. 4, panel b) and was confirmed by WB analysis (Fig. 5). Statistically significant differences were determined between any single group and the neuromuscular disease controls for each analyzed protein. Thus, in order to distinguish among the groups, more than one altered protein/pathway has to be considered.

A limitation of our study is related to the use of patient fibroblasts. Indeed, our results should be confirmed on muscle biopsies which are the target tissue of laminopathies. However, such a study on muscle biopsy can introduce big issues concerning the heterogeneity of cell types present in there.

As discussed above, the number of patients analyzed, which depends on the rarity of the disease, was very small, impairing the possibility to draw definitive correlations between different phenotypes and protein profiles. The limited number of patients was likely determining that no acceptable clustering was possible, considering other variables, such as clinical phenotype, onset of disease or point mutation localization in recognized lamin domains (data not shown).

In conclusion, we think that our study can contribute to better understand the molecular mechanisms of these rare diseases and eventually facilitate the definition of potential drug targets to develop novel therapies.

Supplementary materials related to this article can be found online at doi:10.1016/j.bbadis.2012.01.014.

Acknowledgements

We are grateful to all patients for collaboration. We would thank Dr Emanuele Alpi for his help in Gene Ontology enrichment analysis and Dr Daniela Gabellini for culturing skin fibroblasts.

The experiments comply with the Italian current laws. The authors declare that they have no conflict of interest.

References

[1] G. Bonne, M.R. Di Barletta, S. Varnous, H.M. Bécane, E.H. Hammouda, L. Merlini, F. Muntoni, C.R. Greenberg, F. Gary, J.A. Urtizberea, D. Duboc, M. Fardeau, D. Toniolo, K. Schwartz, Mutations in the gene encoding Lamin A/C cause autosomal dominant Emery–Dreifuss muscular dystrophy, Nat. Genet. 21 (1999) 285–288.

[2] A. Muchir, G. Bonne, A.J. van der Kooi, M. van Meegen, F. Baas, P.A. Bolhuis, M. de Visser, K. Schwartz, Identification of mutations in the gene encoding Lamins A/C in autosomal dominant limb girdle muscular dystrophy with atrioventricular conduction disturbances (LGMD1B), Hum. Mol. Genet. 9 (2000) 1453–1459.

[3] A. De Sandre-Giovannoli, M. Chaouch, S. Kozlov, J.M. Vallat, M. Tazir, N. Kassouri, P. Szepetowski, T. Hammadouche, A. Vandenberghe, C.L. Stewart, D. Grid, N. Lévy, Homozygous defects in LMNA, encoding Lamin A/C nuclear-envelope proteins, cause autosomal recessive axonal neuropathy in human (Charcot–Marie–Tooth disorder type 2) and mouse, Am. J. Hum. Genet. 70 (2002) 726–736.

[4] D. Fatkin, C. MacRae, T. Sasaki, M.R. Wolff, M. Porcu, M. Frenneaux, J. Atherton, H.J. Jr Vidaillet, S. Spudich, U. De Girolami, J.G. Seidman, C. Seidman, F. Muntoni, G. Müehle, W. Johnson, B. McDonough, Missense mutations in the rod domain of the Lamin A/C gene as causes of dilated cardiomyopathy and conductionsystem disease, N. Engl. J. Med. 341 (1999) 1715–1724.
[5] H. Cao, R.A. Hegele, Nuclear Lamin A/C R482Q mutation in Canadian kindreds with Dunnigan-type familial partial lipodystrophy, Hum. Mol. Genet. 9 (2000) 109–112.
[6] G. Novelli, A. Muchir, F. Sangiuolo, A. Helbling-Leclerc, M.R. D'Apice, C. Massart, F. Capon, P. Sbraccia, M. Federici, R. Lauro, C. Tudisco, R. Pallotta, G. Scarano, B. Dallapiccola, L. Merlini, G. Bonne, Mandibuloacral dysplasia is caused by a mutation in *LMNA*-encoding Lamin A/C, Am. J. Hum. Genet. 71 (2002) 426–431.
[7] A. De Sandre-Giovannoli, R. Bernard, P. Cau, C. Navarro, J. Amiel, I. Boccaccio, S. Lyonnet, C.L. Stewart, A. Munnich, M. Le Merrer, N. Lévy, Lamin a truncation in Hutchinson–Gilford progeria, Science 300 (2003) 2055.
[8] C.L. Navarro, De A. Sandre-Giovannoli, R. Bernard, I. Boccaccio, A. Boyer, D. Geneviève, S. Hadj-Rabia, C. Gaudy-Marqueste, H.S. Smitt, P. Vabres, L. Faivre, A. Verloes, T. Van Essen, E. Flori, R. Hennekam, F.A. Beemer, N. Laurent, M. Le Merrer, P. Cau, N. Lévy, Lamin A and ZMPSTE24 (FACE-1) defects cause nuclear disorganization and identify restrictive dermopathy as a lethal neonatal laminopathy, Hum. Mol. Genet. 13 (2004) 2493–2503.
[9] S. Benedetti, I. Menditto, M. Degano, C. Rodolico, L. Merlini, A. D'Amico, L. Palmucci, A. Berardinelli, E. Pegoraro, C.P. Trevisan, L. Morandi, I. Moroni, G. Galluzzi, E. Bertini, A. Toscano, M. Olivè, G. Bonne, F. Mari, R. Caldara, R. Fazio, I. Mammì, P. Carrera, D. Toniolo, G. Comi, A. Quattrini, M. Ferrari, S.C. Previtali, Phenotypic clustering of lamin A/C mutations in neuromuscular patients, Neurology 69 (2007) 1285–1292.
[10] J. Lammerding, P.C. Schulze, T. Takahashi, S. Kozlov, T. Sullivan, R.D. Kamm, C.L. Stewart, R.T. Lee, Lamin A/C deficiency causes defective nuclear mechanics and mechanotransduction, J. Clin. Invest. 113 (2004) 370–378.
[11] V. Nikolova, C. Leimena, A.C. McMahon, J.C. Tan, S. Chandar, D. Jogia, S.H. Kesteven, J. Michalicek, R. Otway, F. Verheyen, S. Rainer, C.L. Stewart, D. Martin, M.P. Feneley, D. Fatkin, Defects in nuclear structure and function promote dilated cardiomyopathy in Lamin A/C-deficient mice, J. Clin. Invest. 113 (2004) 357–369.
[12] D.K. Shumaker, E.R. Kuczmarski, R.D. Goldman, The nucleoskeleton: lamins and actin are major players in essential nuclear functions, Curr. Opin. Cell Biol. 15 (2003) 358–366.
[13] V. Stierlé, J. Couprie, C. Ostlund, I. Krimm, S. Zinn-Justin, P. Hossenlopp, H.J. Worman, J.C. Courvalin, I. Duband-Goulet, The carboxyl-terminal region common to lamins A and C contains a DNA binding domain, Biochemistry 42 (2003) 4819–4828.
[14] A. Muchir, P. Pavlidis, G. Bonne, Y.K. Hayashi, H.J. Worman, Activation of MAPK in hearts of EMD null mice: similarities between mouse models of X-linked and autosomal dominant Emery Dreifuss muscular dystrophy, Hum. Mol. Genet. 16 (2007) 1884–1895.
[15] A. Muchir, P. Pavlidis, V. Decostre, A.J. Herron, T. Arimura, G. Bonne, H.J. Worman, Activation of MAPK pathways links LMNA mutations to cardiomyopathy in Emery–Dreifuss muscular dystrophy, J. Clin. Invest. 117 (2007) 1282–1293.
[16] M. Bakay, Z. Wang, G. Melcon, L. Schiltz, J. Xuan, P. Zhao, V. Sartorelli, J. Seo, E. Pegoraro, C. Angelini, B. Shneiderman, D. Escolar, Y.W. Chen, S.T. Winokur, L.M. Pachman, C. Fan, R. Mandler, Y. Nevo, E. Gordon, Y. Zhu, Y. Dong, Y. Wang, E.P. Hoffman, Nuclear envelope dystrophies show a transcriptional fingerprint suggesting disruption of Rb-MyoD pathways in muscle regeneration, Brain 129 (2006) 996–1013.
[17] V. Andrés, J.M. González, Role of A-type lamins in signaling, transcription, and chromatin organization, J. Cell Biol. 187 (2009) 945–957.
[18] A. Méjat, V. Decostre, J. Li, L. Renou, A. Kesari, D. Hantaï, C.L. Stewart, X. Xiao, E. Hoffman, G. Bonne, T. Misteli, Lamin A/C-mediated neuromuscular junction defects in Emery–Dreifuss muscular dystrophy, J. Cell Biol. 84 (2009) 31–44.
[19] V.F. Gnocchi, J.A. Ellis, P.S. Zammit, Does satellite cell dysfunction contribute to disease progression in Emery–Dreifuss muscular dystrophy? Biochem. Soc. Trans. 36 (2008) 1344–1349.
[20] H.J. Worman, G. Bonne, "Laminopathies": a wide spectrum of human diseases, Exp. Cell Res. 313 (2007) 2121–2133.
[21] P. Doran, P. Donoghue, K. O'Connell, J. Gannon, K. Ohlendieck, Proteomic profiling of pathological and aged skeletal muscle fibres by peptide mass fingerprinting, Int. J. Mol. Med. 19 (2007) 547–564.
[22] C. Lewis, H. Jockusch, K. Ohlendieck, Proteomic profiling of the dystrophin-deficient MDX heart reveals drastically altered levels of key metabolic and contractile proteins, J. Biomed. Biotechnol. 2010 (2010) ID 648501.
[23] S. Benedetti, E. Bertini, S. Iannaccone, C. Angelini, M. Trisciani, D. Toniolo, B. Sferrazza, P. Carrera, G. Comi, M. Ferrari, A. Quattrini, S.C. Previtali, Dominant *LMNA* mutations can cause combined muscular dystrophy and peripheral neuropathy, J. Neurol. Neurosurg. Psychiatry 76 (2005) 1019–1021.
[24] R. Westermeier, R. Marouga, Protein detection methods in proteomics research, Biosci. Rep. 25 (2005) 19–32.
[25] A. Shevchenko, M. Wilm, O. Vorm, M. Mann, Mass spectrometric sequencing of proteins silver-stained polyacrylamide gels, Anal. Chem. 68 (1996) 850–858.
[26] C. Magagnotti, I. Fermo, R.M. Carletti, M. Ferrari, A. Bachi, Comparison of different depletion strategies for improving resolution of the human urine proteome, Clin. Chem. Lab. Med. 48 (2010) 531–535.
[27] V. Matafora, A. D'Amato, S. Mori, F. Blasi, A. Bachi, Proteomics analysis of nucleolar SUMO-1 target proteins upon proteasome inhibition, Mol. Cell. Proteomics 8 (2009) 2243–2255.
[28] J.Y. King, R. Ferrara, R. Tabibiazar, J.M. Spin, M.M. Chen, A. Kuchinsky, A. Vailaya, R. Kincaid, A. Tsalenko, D.X. Deng, A. Connolly, P. Zhang, E. Yang, C. Watt, Z. Yakhini, A. Ben-Dor, A. Adler, L. Bruhn, P. Tsao, T. Quertermous, E.A. Ashley, Pathway analysis of coronary atherosclerosis, Physiol. Genomics 23 (2005) 103–118.
[29] S. Maere, K. Heymans, M. Kuiper, BiNGO: a Cytoscape plugin to assess overrepresentation of gene ontology categories in biological networks, Bioinformatics 21 (2005) 3448–3449.
[30] L. Eriksson, E. Johansson, N. Kettaneh-Wold, S. Wold, Introduction to the Multi- and Megavariate Data Analysis Using Projection Methods (PCA & PLS), first ed Umetrics AB, Umea,Sweden, 1999.
[31] C. Favreau, E. Dubosclard, C. Ostlund, C. Vigouroux, J. Capeau, M. Wehnert, D. Higuet, H.J. Worman, J.C. Courvalin, B. Buendia, Expression of lamin A mutated in the carboxyl-terminal tail generates an aberrant nuclear phenotype similar to that observed in cells from patients with Dunnigan-type partial lipodystrophy and Emery–Dreifuss muscular dystrophy, Exp. Cell Res. 282 (2003) 14–23.
[32] K. Bechert, M. Lagos-Quintana, J. Harborth, K. Weber, M. Osborn, Effects of expressing lamin A mutant protein causing Emery–Dreifuss muscular dystrophy and familial partial lipodystrophy in HeLa cells, Exp. Cell Res. 286 (2003) 75–86.
[33] S. Chen, C. Martin, A. Maya-Mendoza, C.W. Tang, J. Lovrić, P.F. Sims, D.A. Jackson, Reduced expression of Lamin A/C results in modified cell signaling and metabolism coupled with changes in expression of structural proteins, J. Proteome Res. 8 (2009) 5196–5211.
[34] C.L. Stewart, S. Kozlov, L.G. Fong, S.G. Young, Mouse models of the laminopathies, Exp. Cell Res. 313 (2007) 2144–2156.
[35] G. Novelli, M.R. D'Apice, The strange case of the "lumper" Lamin A/C gene and human premature ageing, Trends Mol. Med. 9 (2003) 370–375.
[36] C. Vigouroux, M. Auclair, E. Dubosclard, M. Pouchelet, J. Capeau, J.C. Courvalin, B. Buendia, Nuclear envelope disorganization in fibroblasts from lipodystrophic patients with heterozygous R482Q/W mutations in the Lamin A/C gene, J. Cell Sci. 114 (2001) 4459–4468.
[37] J.L. Broers, E.A. Peeters, H.J. Kuijpers, J. Endert, C.V. Bouten, C.W. Oomens, F.P. Baaijens, F.C. Ramaekers, Decreased mechanical stiffness in LMNA$^{-/-}$ cells is caused by defective nucleo-cytoskeletal integrity: implications for the development of laminopathies, Hum. Mol. Genet. 13 (2004) 2567–2580.
[38] J.S. Lee, C.M. Hale, P. Panorchan, S.B. Khatau, J.P. George, Y. Tseng, C.L. Stewart, D. Hodzic, D. Wirtz, Nuclear Lamin A/C deficiency induces defects in cell mechanics, polarization, and migration, Biophys. J. 93 (2007) 2542–2552.
[39] E.S. Folker, C. Ostlund, G.W. Luxton, H.J. Worman, G.G. Gundersen, Lamin A variants that cause striated muscle disease are defective in anchoring transmembrane actin-associated nuclear lines for nuclear movement, Proc. Natl. Acad. Sci. 108 (2011) 131–136.
[40] J.L. Broers, F.C. Ramaekers, G. Bonne, R.B. Yaou, C.J. Hutchison, Nuclear lamins: laminopathies and their role in premature ageing, Physiol. Rev. 86 (2006) 967–1008.
[41] C.M. Hale, A.L. Shrestha, S.B. Khatau, P.J. Stewart-Hutchinson, L. Hernandez, C.L. Stewart, D. Hodzic, D. Wirtz, Dysfunctional connections between the nucleus and the actin and microtubule networks in laminopathic models, Biophys. J. 95 (2008) 5462–5475.
[42] S. Chen, C. Martin, A. Maya-Mendoza, C.W. Tang, J. Lovrić, P.F. Sims, D.A. Jackson, Reduced expression of lamin A/C results in modified cell signaling and metabolism coupled with changes in expression of structural proteins, J. Proteome Res. 8 (2009) 5196–5211.
[43] M. Boschmann, S. Engeli, C. Moro, A. Luedtke, F. Adams, K. Gorzelniak, G. Rahn, A. Mähler, K. Dobberstein, A. Krüger, S. Schmidt, S. Spuler, F.C. Luft, S.R. Smith, H.H. Schmidt, J. Jordan, *LMNA* mutations, skeletal muscle lipid metabolism, and insulin resistance, J. Clin. Endocrinol. Metab. 95 (4) (2010) 1634–1643.
[44] J.G. Tidball, M. Wehling-Henricks, The role of free radicals in the pathophysiology of muscular dystrophy, J. Appl. Physiol. 102 (2007) 1677–1686.
[45] J.C. Charniot, D. Bonnefont-Rousselot, C. Marchand, K. Zerhouni, N. Vignat, J. Peynet, M. Plotkine, A. Legrand, J.Y. Artigou, Oxidative stress implication in a new phenotype of amyotrophic quadricipital syndrome with cardiac involvement due to lamin A/C mutation, Free. Radic. Res. 41 (2007) 424–431.
[46] V.L. Verstraeten, S. Caputo, M.A. van Steensel, I. Duband-Goulet, S. Zinn-Justin, M. Kamps, H.J. Kuijpers, C. Ostlund, H.J. Worman, J.J. Briedé, C. Le Dour, C.L. Marcelis, M. van Geel, P.M. Steijlen, A. van den Wijngaard, F.C. Ramaekers, J.L. Broers, The R439C mutation in LMNA causes lamin oligomerization and susceptibility to oxidative stress, J. Cell. Mol. Med. 13 (2009) 959–971.